Room-temperature ferromagnetism in Ca and Mg stabilized cubic zirconia bulk samples and thin films prepared by pulsed laser deposition

2012 J. Phys. D: Appl. Phys. 45 475003

(http://iopscience.iop.org/0022-3727/45/47/475003)

J. Phys. D: Appl. Phys. **45** (2012) 475003 (7pp) doi:10.1088/0022-3727/45/47/475003

Room-temperature ferromagnetism in Ca and Mg stabilized cubic zirconia bulk samples and thin films prepared by pulsed laser deposition

M Chandra Dimri[1], H Khanduri[1,2], H Kooskora[1], M Kodu[3], R Jaaniso[3], I Heinmaa[1], A Mere[2], J Krustok[2] and R Stern[1]

[1] National Institute of Chemical Physics and Biophysics, Tallinn-12618, Estonia
[2] Department of Physics, Faculty of Science, Tallinn University of Technology, Tallinn-19086, Estonia
[3] Institute of Physics, Faculty of Science and Technology, University of Tartu, EE-51014, Tartu, Estonia

E-mail: mukeshdimri@yahoo.com

Received 20 June 2012, in final form 2 October 2012
Published 1 November 2012
Online at stacks.iop.org/JPhysD/45/475003

Abstract
We report room-temperature ferromagnetism in Ca and Mg stabilized zirconia bulk samples and thin films. Powders were prepared by the citrate-combustion route, and thin films grown on silicon substrates by the pulsed laser deposition technique. X-ray diffractograms and Raman spectra at room temperature reveal the formation of cubic phase zirconia. The observed ferromagnetism is robust at room temperature in both bulk as well as in thin film samples, although it is weaker in thin films. The origin of the ferromagnetism can be related to oxygen vacancies created due to divalent (calcium and magnesium) substitution for tetravalent zirconium ions.

(Some figures may appear in colour only in the online journal)

1. Introduction

Dilute magnetic semiconductors (DMS) have attracted vast interest in the last decade because of the possibility of assembling charge and spin degrees of freedom in a single substance. That makes them promising candidates for technological applications in spintronic devices, utilizing both the electronic charge as well as their spins [1–3]. With this hope to realize spintronic devices such as spin valves, spin transistors, spin light-emitting diodes (LEDs), ultrafast optical switches, etc, a significant amount of research effort has been focused on discovering materials suitable for these applications. A large number of transition metal (TM) doped oxides have been examined since the first prediction of ferromagnetism in Mn-doped ZnO by Dietl *et al* in 2000 [2]. A remarkable amount of research has been carried out to understand the nature of magnetism in TM-doped oxide systems, such as ZnO, TiO_2, HfO_2, CeO_2, SnO_2 and In_2O_3 [4–9]. However, the experimental search for ferromagnetism in TM-doped oxide materials has not yet resulted in reproducible and homogeneous magnetic materials.

Interestingly, ferromagnetism has been suggested to be possible even in systems that do not contain magnetic impurities, materials often referred to as d^0 or intrinsic ferromagnets [10, 11]. Experimentally, it has been shown that thin films of HfO_2 and ZnO [12, 13] exhibit such type of ferromagnetism with a rather high Curie temperature (T_C). The ferromagnetism with high Curie temperature was also proposed by substitution of the four-valent cation A^{4+} in dioxides such as AO_2 (A = Ti, Zr, or Hf) by a monovalent cation of group 1A of the periodic table [11]. HfO_2 and ZrO_2 are both wide-band insulating materials with a high dielectric constant; the possibility of making them ferromagnetic could widen their possible application in the emerging field of spintronics.

Recent theoretical studies also predicted high-temperature ferromagnetism in TM-doped cubic zirconia [14] and K-doped ZrO_2 [11]. However, doping with Cu [15], Cr [14] or Ca

[11] in ZrO_2 can result in paramagnetism, antiferromagnetic or non-magnetic ground states, respectively. According to these theories, single oxygen vacancy induces local magnetic moments on the neighbouring oxygen atoms, which then interact with extended exchange coupling. Motivated by these promising theoretical predictions of ferromagnetism in doped ZrO_2, a few experimental works have been carried out to confirm the room-temperature ferromagnetism in $Zr_{1-x}Mn_xO_2$ [16–18] and $Zr_{1-x}Fe_xO_2$ [19]. However, experimental results were controversial in these studies, and ferromagnetism was not shown up to the level, which has been predicted. Our recent experimental study on Mn-doped ZrO_2 [17] suggested that an undesired secondary phase like Mn_3O_4 segregates on high-temperature heat treatments. To overcome the problems related to secondary phases, we study further the possibility of ferromagnetism in ZrO_2 stabilized with non-magnetic elements such as Ca or Mg, as they are well soluble in the zirconia matrix and their magnetic properties have not yet been investigated experimentally.

In this paper, we report the ferromagnetic properties observed in cubic zirconia stabilized with non-magnetic dopants (Ca, Mg and Y). Accordingly, we synthesized bulk and thin films of Ca, Y and Mg stabilized cubic zirconia, and studied their structural and magnetic properties to understand the dopant effects. Optimum dopant concentrations (16 at% Ca and 14 at% Mg in ZrO_2) were selected from the phase diagrams reported in the literature to get the cubic crystalline phase at room temperature [20, 21]. Y-stabilized cubic zirconia (YSZ) samples were found to be paramagnetic, so the results are not discussed in this paper.

2. Experimental

Polycrystalline powders of $Zr_{1-x}Ca_xO_2$ ($x = 0$ and 0.16) and $Zr_{0.86}Mg_{0.14}O_2$ were prepared by the chemical citrate-combustion route [17]. Zirconyl oxychloride ($ZrOCl_2{\cdot}8H_2O$), CaO and MgO were used as starting materials. 0.5M solutions were prepared in deionized water for zirconium salt, whereas CaO and MgO were dissolved in excess of nitric acid and peroxide. Citric acid was added in 3 : 2 proportions for every cation. The resulting solution after mixing was first heated at 60 °C for 2 h and later at 80 °C till the complete evaporation of solvents. All our as-prepared powders were calcined at 800 °C in air for 5 h. To see the effects of annealing in other environments than air, the as-prepared powder samples were alternatively calcined in argon/hydrogen environments at 800 °C/5 h. The calcined powders were pressed to disc-shaped pellets and sintered in air at either 1200 or 1500 °C for 3 h, to investigate the dependence of structural and magnetic properties on sintering temperatures.

Thin films of 16 at% calcium-doped ZrO_2 were deposited on 10×10 mm Si (1 0 0)/SiO_2 (25 nm thermal oxide) substrates by the pulsed laser deposition (PLD) technique. The substrates were ultrasonically cleaned in an acetone bath prior to the deposition process. Pellets that were used as PLD targets were sintered at 1200 °C for 5 h. A KrF excimer laser (COMPexPro 205, Coherent, wavelength 248 nm, pulse width 25 ns) was used for ablation. The deposition conditions of the $Zr_{1-x}Ca_xO_2$ films were as follows: laser pulse energy density on the target 2 J cm^{-2}, repetition rate of laser 5 Hz, substrate temperature 800 °C, the distance between the substrate and the target 7.5 cm. Ca-doped ZrO_2 thin films were deposited at three different oxygen pressures in the chamber during the film growth: 10^{-2}, 10^{-3} and 10^{-4} mbar. The number of laser impulses for growing each film were 30 000 and the resulting thicknesses of the films were ∼150 nm.

The x-ray diffraction technique (Rigaku Ultima IV) and Raman spectroscopy (Horiba Jobin Yvon LabRAM HR 800) were used for structural identification at room temperature, whereas magnetic measurements were performed using a vibrating sample magnetometer (14 T PPMS-Quantum Design). Scanning electron micrographs (SEM) for microstructure and energy dispersive spectroscopic (EDS) measurements for stoichiometry were also made for those samples using a Zeiss EVO-MA15 apparatus.

3. Results and discussion

X-ray diffraction patterns for the undoped as well as Ca- and Mg-doped ZrO_2 bulk samples, heated at different temperatures are shown in figure 1(*a*). From these diffractograms we see that 16 at% Ca- and 14 at% Mg-doped ZrO_2 samples sintered at 1500 °C exhibit a pure cubic (C) zirconia phase. The undoped sample sintered at 800 °C shows a monoclinic structure with an extra peak of tetragonal zirconia, whereas a single-phase monoclinic structure is exhibited by the sample sintered at 1500 °C. The lower, 10 at% Ca-doped zirconia sample shows a mixed cubic and tetragonal (T) structure; the presence of the tetragonal structure in this sample is also confirmed by the Raman spectra (figure not included). Figure 1(*b*) shows the diffractograms for the PLD thin films of the 16 at% Ca-doped ZrO_2, grown at different oxygen partial pressures. The films show one XRD peak for cubic zirconia (1 1 1) and other intense peaks from the silicon substrate. Raman spectra (see figure 2(*b*)) also confirm the cubic phase formation for thin films showing a characteristic cubic XRD pattern.

Raman spectra measured at room temperature for the bulk and thin film samples of doped zirconia are shown in figures 2(*a*) and (*b*). The spectrum for 16 at% Ca-doped ZrO_2 sintered sample at 1500 °C (figure 2(*a*)) validates the cubic phase formation (Raman peaks around 275, 410, 520 and 580 cm^{-1}) [22], whereas the peaks are not separable for both Ca and Mg stabilized zirconia samples heated at 800 °C. These broad and flat spectra may be related to the mixed zirconia phases at 800 °C, although XRD could show single phase for those powders. Usually, the strongest Raman peak position is around 615 cm^{-1} for yttria-stabilized zirconia samples [22], but for Ca-stabilized zirconia this shifts towards lower values, and it is around 580 cm^{-1} in our sample. This shift may be because of the difference in sizes and mass of Ca and Zr, as compared with Y and Zr [22]. Raman spectra for the PLD thin films of 16% Ca-doped ZrO_2 demonstrate characteristic peaks of cubic zirconia (155, 425, 620 cm^{-1}); the strong peaks due to the silicon substrate (near 300 and 530 cm^{-1}) can also be seen in the spectra that suppress the

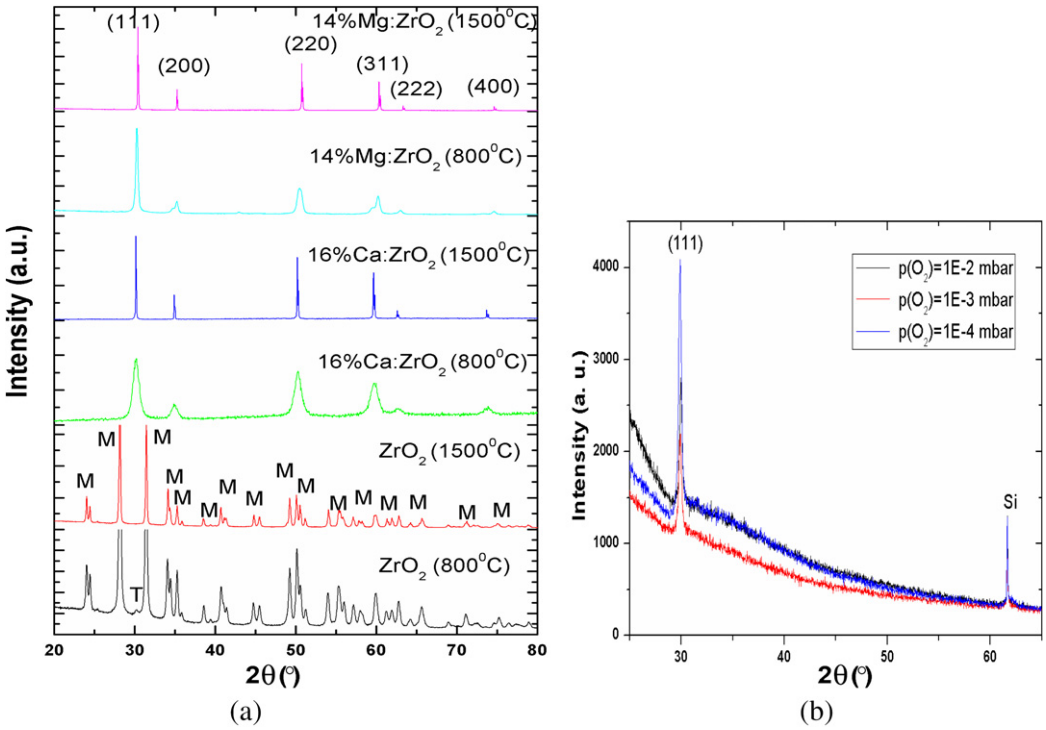

Figure 1. XRD patterns of (*a*) bulk powders heat-treated at different temperatures, (*b*) 16% Ca-doped ZrO_2 thin films deposited at various oxygen partial pressures.

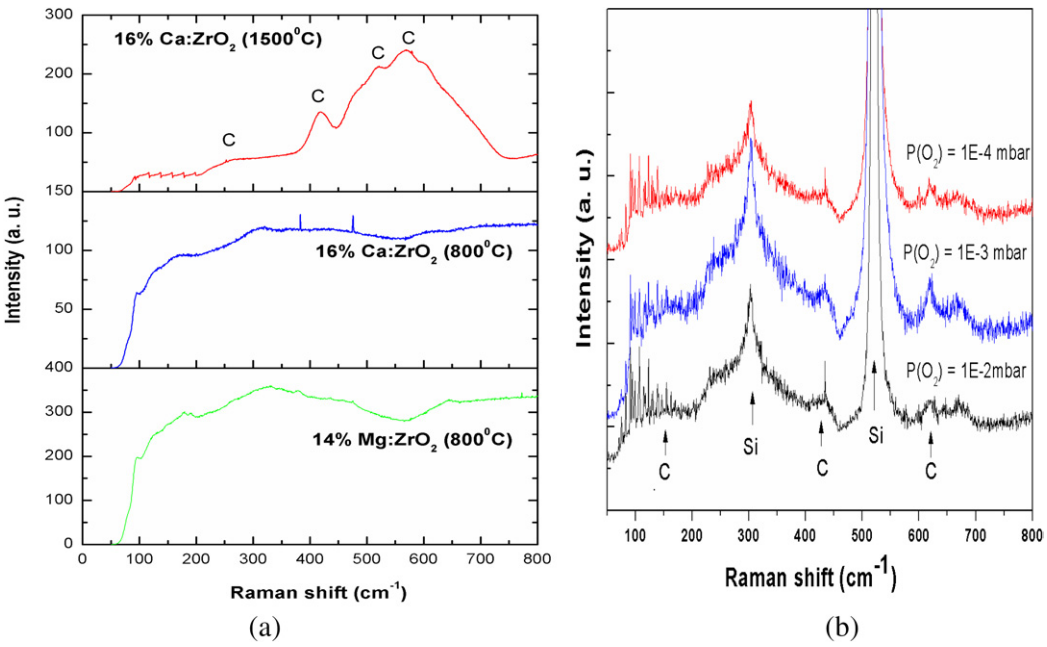

Figure 2. Room-temperature Raman spectra of (*a*) bulk samples of doped ZrO_2; (*b*) $Zr_{0.84}Ca_{0.16}O_2$ thin films.

intensity of zirconia modes. Our results are consistent with another Raman study by Gazzoli *et al* [23], which showed that above 14% calcium doping stabilizes the cubic zirconia phase and below this doping concentration it results in a tetragonal structure; we have also observed the Raman spectra resembling the tetragonal structure for 10 at% Ca^{2+} in ZrO_2 (figure not included).

SEM micrographs and EDX spectra of the undoped and doped zirconia samples sintered at different temperatures are shown in figure 3. The EDX spectra reveal that the chemical compositions are in good agreement with the desired stoichiometry, and there are no impurities in the prepared samples. From the SEM images we can visualize that all those samples have grains in the micrometre (μm) range; however, the grains are smaller ($\sim$2–5 μm) for the samples treated at 800 °C and the undoped sintered sample at 1500 °C, whereas the grains are in the range 3–8 μm for the doped sintered samples at 1500 °C.

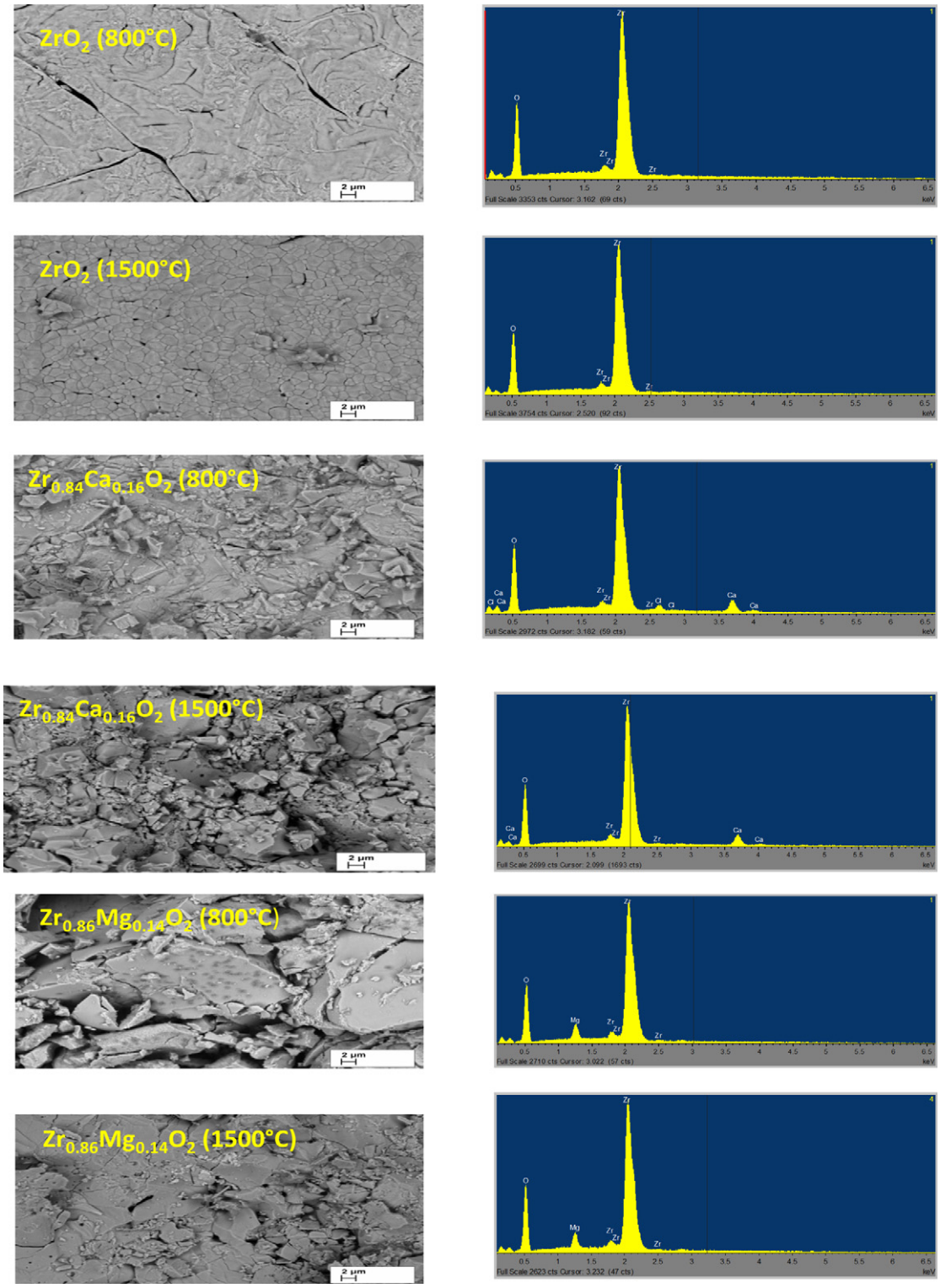

Figure 3. SEM micrographs and EDX spectra of the undoped and doped zirconia samples.

Hysteresis loops measured at room temperature (300 K) for the Ca- and Mg-doped and undoped ZrO_2 samples heated at 800 and 1500 °C are shown in figure 4. M–H loops of the doped zirconia samples appear like a good ferromagnet for the powders heated at 800 °C, whereas the diamagnetism is enhanced in samples sintered at higher temperatures. The enhancement of the diamagnetic signal in the sintered samples may be due to the decrease in the number of oxygen vacancies on high-temperature treatment in air. The coercivities and spontaneous magnetization (at 0.5 T) estimated from these curves are listed in table 1. There are no remarkable changes in coercivities, whereas the saturation magnetization decreases with the increase in sintering temperatures. The undoped ZrO_2 samples also exhibit tiny ferromagnetic hysteresis, possibly

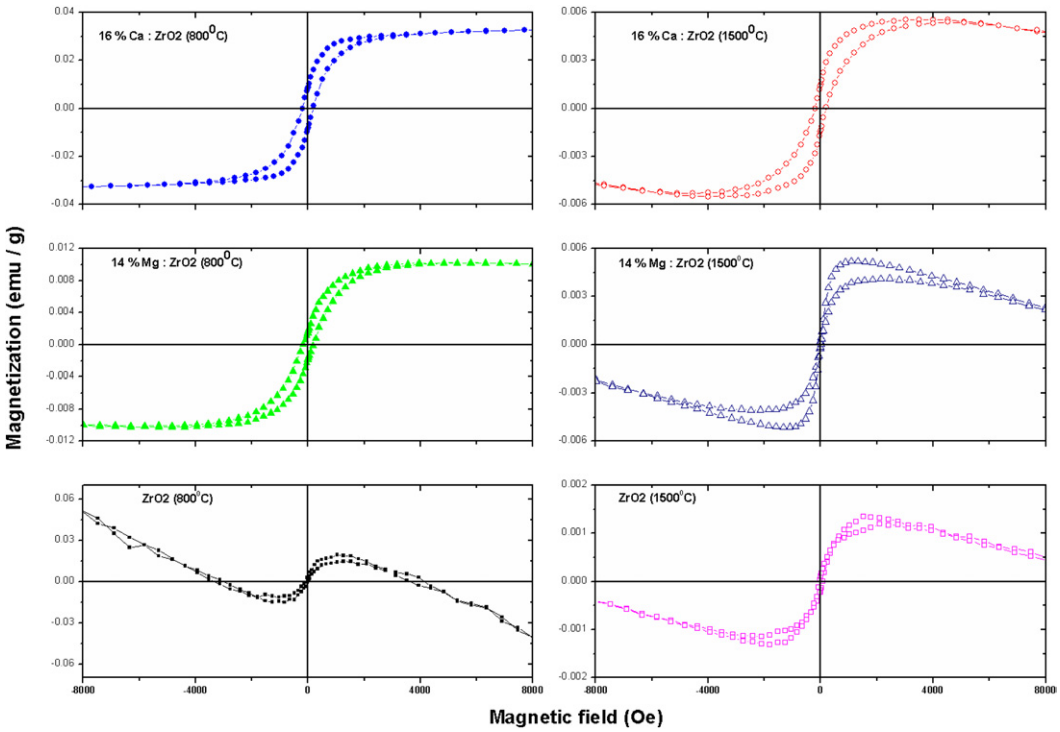

Figure 4. As-measured ($T = 300$ K) hysteresis loops of Ca- and Mg-doped ZrO_2 bulk samples heated at 800 and 1500 °C.

Table 1. Magnetic parameters for different Ca- and Mg-doped zirconia samples.

	$Zr_{0.84}Ca_{0.16}O_2$			$Zr_{0.86}Mg_{0.14}O_2$	
	800 °C	1200 °C	1500 °C	800 °C	1200 °C
M_s in emu g^{-1} (at 0.5 T)	0.0335	0.0076	0.0055	0.012	0.005
Coercivity (Oe)	200	200	200	185	25

due to the presence of some oxygen vacancies in our samples. The density of oxygen vacancies is strongly dependent on the synthesis methods [24]. Zirconyl oxychloride was used as the zirconium precursor, so there is excess chlorine (Cl_2) during the sintering process, which was reported in an old study [24], which showed that preparation by nitrate or oxychloride precursors leads to oxygen vacancies in zirconia; however the vacancies are lower in the samples prepared by oxychloride precursors. This is confirmed from the weak ferromagnetic signal in M–H measurements (figure 4) due to these oxygen vacancies; however, the oxygen vacancy concentration was not enough to result in long-range ferromagnetic ordering in these undoped samples.

Figure 5 shows the M–H curves measured at room temperature (300 K) for the $Zr_{0.84}Ca_{0.16}O_2$ bulk samples annealed at 800, 1200 and 1500 °C/3 h in air. The magnetization decreases with increase in the sintering temperature, whereas the coercivity does not change noticeably. Saturation magnetization is six times larger for the sample annealed at 800 °C, as compared with the sample treated at 1500 °C. These results suggest that vacancies present at lower temperatures enhance the ferromagnetism, which

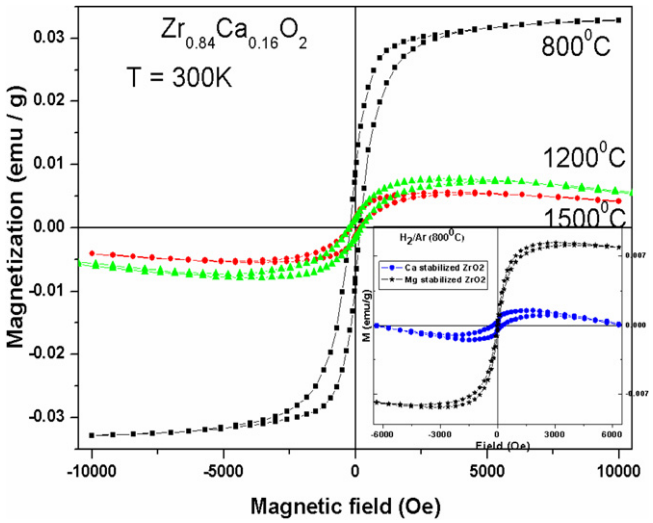

Figure 5. Hysteresis loops (measured at room temperature) of the $Zr_{0.84}Ca_{0.16}O_2$ bulk samples sintered at different temperatures in air.

diminishes on high-temperature treatments. The decrease in oxygen vacancies on high-temperature treatments results in the lowering of the ferromagnetic order and magnetic moment. There are more vacancies at 800 °C, due to the mixed phase (tetragonal phase as an additional phase), also reported in another study [25]. The decrease in oxygen vacancies on high-temperature treatments are also observed in other studies conducted for photoluminescence [26, 27]. The inset shows the M–H loops of the Ca- and Mg-doped ZrO_2 samples annealed in a H_2/argon environment. In order to examine the defect nature of magnetism, annealing in different environments was performed, but even annealing in H_2/Ar

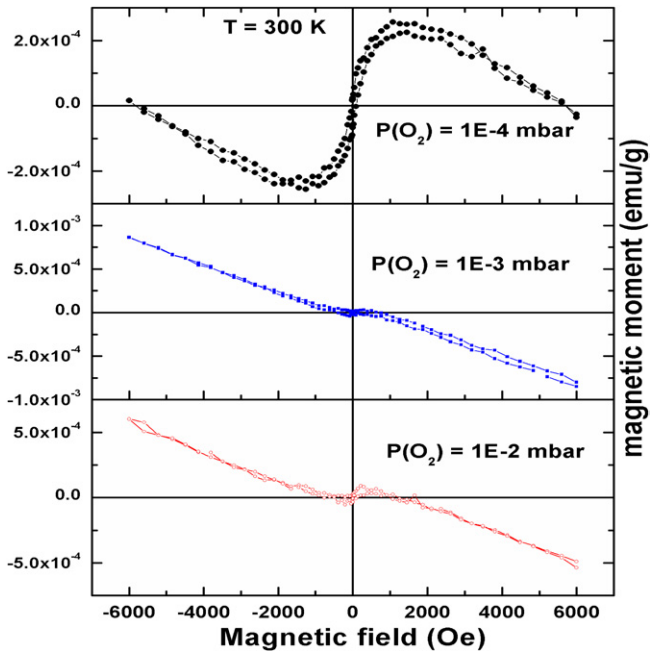

Figure 6. M–H loops measured (room temperature) for the thin films of $Zr_{0.84}Ca_{0.16}O_2$ samples grown at different oxygen pressures.

environment could not enhance the long-range ferromagnetic ordering at high temperatures, as expected due to the increasing number of oxygen vacancies. The temperature dependence of magnetization for these samples was also measured in the temperature range 10–350 K (figures not included); it was almost constant and did not show any transition in this temperature range.

Figure 6 shows the dependence of magnetization on the magnetic field at room temperature for $Zr_{0.84}Ca_{0.16}O_2$ thin films, grown on silicon substrates with different oxygen pressures. The ferromagnetic ordering is quite weak for samples grown at oxygen partial pressures of 10^{-2} and 10^{-3} mbar, whereas the film grown at an oxygen partial pressure of 10^{-4} mbar shows ferromagnetic character. This indicates that the film grown at lower oxygen partial pressures has more oxygen vacancies, available for ferromagnetic ordering. This type of oxygen partial pressure dependence was also observed in doped ZnO and SnO_2 oxide thin films by Hong *et al*, and in CeO_2 by Singhal *et al* [28, 29]. There are often significant differences between the properties of bulk samples and thin films due to the effects of the substrate; the magnetic moments are quite low in the thin film samples, as expected. The magnetization does not saturate due to the dominating diamagnetic signal from the silicon substrate, but the value of spontaneous magnetization (M) $\sim 2 \times 10^{-4}$ emu g^{-1} (at 2000 Oe) and the coercivity is around 80 Oe, and those values are quite low as compared with bulk values (see table 1).

Usually, bulk ZrO_2 is diamagnetic at room temperature. When Ca^{2+} or Mg^{2+} ions are substituted for zirconium ion (Zr^{4+}) sites, compensating anionic vacancies are created in the O^{2-} sublattice. These anionic vacancies could be the origin of ferromagnetism in non-magnetic divalent ion doped ZrO_2. This type of defect induced magnetism has already been observed in thin films of undoped HfO_2, TiO_2 [12, 30] and many other nanoparticles [31, 32], usually found in thin films and nanoparticles due to surface effects. However, this type of ferromagnetism in our bulk samples is robust and repeatable (even after months), because the samples are highly crystalline cubic zirconia, obtained on heating at very high temperatures. High-temperature treatments and larger grains ruled out the possibilities of hygroscopic nature and ageing, which have been observed in our recent study on Mn-doped zirconia powders due to low-temperature treatments and nano-sized grains [17].

4. Conclusions

In conclusion, we have observed room-temperature ferromagnetism in Ca and Mg stabilized zirconia bulk samples and similar thin film oriented in [111] direction. X-ray diffraction studies and Raman spectra measured at room temperature reveal the formation of cubic phase zirconia. Bulk powders show good ferromagnetic hysteresis loops, whereas it is weaker in thin films. The origin of the ferromagnetism can be related to oxygen vacancies created due to divalent calcium and magnesium ion substitution for tetravalent zirconium ions.

Acknowledgments

This work was financially supported by the Estonian Science Foundation (grant numbers: MJD 65 and ETF 8440), and the Estonian targeted financial grants SF0690029s09 and SF0690034s09. Part of this study was also supported by the European Union through the European Regional Development Fund (Centre of Excellence ‘Mesosystems: Theory and Applications’, TK114).

References

[1] Ohno H 1998 *Science* **281** 951
[2] Dietl T, Ohno H, Matsukura F, Cibert J and Ferrand D 2000 *Science* **287** 1019
[3] Matsumoto Y, Murakami M, Shono T, Hasegawa T, Fukumura T, Kawasaki M, Ahmet P, Chikyow T, Koshihara S and Koinuma H 2001 *Science* **291** 854
[4] Sharma P, Gupta A, Rao K V, Owens F J, Sharma R, Ahuja R, Osorio Guillen J M, Johansson B and Gehring G A 2003 *Nature Mater.* **2** 673
[5] Bryan J D, Heald S M, Chambers S A and Gamelin D R 2004 *J. Am. Chem. Soc.* **126** 11640
[6] Coey J M D, Venkatesan M, Stamenov P, Fitzgerald C B and Dorneles L S 2005 *Phys. Rev.* B **72** 024450
[7] Wen Q Y, Zhang H W, Song Y Q, Qing-Hui Yang, Hao Zhu and John Q Xiao 2007 *J. Phys.: Condens. Matter.* **19** 246205
[8] Ogale S B *et al* 2003 *Phys. Rev. Lett.* **91** 077205
[9] Philip J, Theodoropoulou N, Berera G, Moodera J S and Satpati B 2004 *Appl. Phys. Lett.* **85** 777
[10] Bouzerar G and Ziman T 2006 *Phys. Rev. Lett.* **96** 207602
[11] Máca F, Kudrnovský J, Drchal V and Bouzerar G 2008 *Appl. Phys. Lett.* **92** 212503
[12] Venkatesan M, Fitzgerald C B and Coey J M D 2004 *Nature* **430** 630
[13] Venkatesan M, Fitzgerald C B, Lunney J G and Coey J M D 2004 *Phys. Rev. Lett.* **93** 177206

[14] Ostanin S, Ernst A, Sandratskii L M, Bruno P, Dane M, Hughes I D, Staunton J B, Hergert W, Mertig I and Kudrnovsky J 2007 *Phys. Rev. Lett.* **98** 016101
[15] Dutta P, Seehra M, Zhang Y and Wender I 2008 *J. Appl. Phys.* **103** 07D104
[16] Yu J, Duan L B, Yang Y C and Rao G H 2008 *Physica* B **403** 4264
[17] Dimri M C, Kooskora H, Pahapill J, Joon E, Heinmaa I, Subbi J and Stern R 2011 *Phys. Status Solidi* a **208** 172
[18] Hong N H, Park C K, Raghavender A T, Ciftja O, Bingham N S, Phan M H and Srikanth H 2012 *J. Appl. Phys.* **111** 07C302
[19] Clavel G, Willinger M G, Zioun D and Pinna N 2008 *Eur. J. Inorg. Chem.* **6** 863–8
[20] Serena S, Sainz M A, Aza S D and Caballero A 2005 *J. Eur. Ceram. Soc.* **25** 681
[21] Stubican V S and Ray S P 1977 *J. Am. Ceram. Soc.* **60** 534
[22] Morell G, Katiyar R S, Torres D, Paje S E and Llopis J 1997 *J. Appl. Phys.* **81** 2830
[23] Gazzoli D, Mattei G and Valigi M 2007 *J. Raman Spectrosc.* **38** 824
[24] Karapetrova E, Platzer R, Gardner J A, Schutfort E, Sommers J A and Evenson W E 2001 *J. Am. Ceram. Soc.* **84** 65
[25] Lu X, Liang K, Gu S, Zheng Y and Fang H 1997 *J. Mater. Sci.* **32** 6653
[26] Xie Y, Ma Z, Liu L, Su Y, Zhao H, Liu Y, Zhang Z, Duan H, Li J and Xie E 2010 *Appl. Phys. Lett.* **97** 141916
[27] Cong Y, Li B, Yue S M, Fan D and Wang X J 2009 *J. Phys. Chem.* C **113** 13974
[28] Hong N H, Sakai J, Huong N T, Poirot N and Ruyter A 2005 *Phys. Rev.* B **72** 045336
[29] Singhal R K, Kumari P, Kumar S, Dolia S N, Xing Y T, Alzamora M, Deshpande U P, Shripathi T and Saitovitch E 2011 *J. Phys. D: Appl. Phys.* **44** 165002
[30] Kim D, Hong J, Park Y R and Kim K J 2009 *J. Phys.: Condens. Matter* **21** 195405
[31] Sundaresan A and Rao C N R 2009 *Nano Today* **4** 96
[32] Coey J M D, Wongsaprom K, Alaria J and Venkatesan M 2008 *J. Phys. D: Appl. Phys.* **41** 134012